Heat Transfer and Thermal Performance of Large-Format Li-ion Battery Modules Employing PCM with Airgap/Aluminum under Extreme Conditions

Abubakar Gambo Mohammed, Karem Elsayed Elfeky, Qiuwang Wang*

Key Laboratory of Thermo-Fluid Science and Engineering, Ministry of Education, School of Energy and Power Engineering, Xi'an Jiaotong University, Xi'an, Shaanxi 710049, P.R. China
wangqw@mail.xjtu.edu.cn

For optimum performance of battery modules in electric vehicles (EVs), the temperature of the batteries must be well managed and maintained within a definite range. In this paper, a passive thermal management with phase change material (PCM) is evaluated for prismatic Li-ion battery modules under abusive conditions. The proposed model aims to analyse the thermal performance of battery modules in circumstances the PCM content is reduced due to a leakage and some part of the batteries are exposed to ambient. Two different configurations are considered: one with the top of the batteries exposed to open medium with free air convection, and the other with the top of the batteries exposed to close medium with no air circulation. Comparing the two configurations, the former decreases the maximum temperature in the module by 1.17 K, 1.39 K, 1.63 K and 1.86 K for 2, 4, 6 and 8 mm PCM shrink levels. The effects of aluminum sheet (Al) placed at the top of the battery modules and charge/discharge cycles were also studied.

1. Introduction

The pollutant emissions caused by internal combustion automobiles is one of the core greenhouse gas (GHG) emission sources. The emission contributes approximately one-fifth to the total carbon dioxide emissions in the European Union (EU) (De Wilde and Kroon, 2013). The adverse effects of the emission gases like nitrogen oxides and carbon dioxides are harmful to human health and environment (Ferrero et al., 2016). In an attempt to regulate and reduce such pollutions and improve air quality, many countries adopted policies of turning the automotive industries into electric vehicles (EVs) and hybrid electric vehicles (HEVs), and considering banning of gasoline cars in some cities (Matthias and Frederic, 2018).

One of the essential component in EVs is the battery, which generate abundant heat during charge and discharge. The energy, performance and power density of the battery module have direct effects on efficiency and driving mileage (Javani et al., 2014). Currently, lithium-ion batteries are considered as the suitable candidate for energy storage in EVs due to their higher energy density, low self-discharge rates and longer cycle life (Ianniciello et al., 2018). However, the stability and performance of the lithium ion batteries are impacted by abnormal temperature rise in the cell or excessive ambient temperature (Luo and Zeng, 2017), that may lead to overheating and deterioration of the entire battery pack. The accumulated heat should be extracted to the ambient to avoid thermal runway and thermal abuse. An effective battery thermal management is significant to maintain the temperature under a specific range and to reduce the excess capacity fading (Wang et al., 2019). Various techniques have been investigated for active, passive, and hybrid battery thermal management. In the year 2000, Al-Hallaj and Selman (2000) proposed a novel thermal management system embedded phase change material for battery use in EVs. A temperature upsurge can significantly be decreased by increasing the thickness of PCM around a battery (Wu et al., 2018). One major drawback of using PCMs as the thermal management system is their low thermal conductivity which leads to slow response in a high demand application (Kim et al., 2019). To address a PCM leakage problem, Li fabricated a composite PCM to prevent leakage during manufacturing (Li et al., 2014). A pyrolytic graphite sheet was introduced to increase the thermal conductivity of the PCM and served as PCM leakage prevention (Wu et al., 2017).

In the present study, thermal performance of a prismatic Li-ion battery module incorporated with PCM partially surrounding the cells is proposed. To illustrate this approach, airgaps at the top of the cells are created. The cooling effectivity is considered for thermal management analysis. The proposed configurations aim to analyze the thermal performance and cooling effectiveness of battery modules in an abusive condition whereby, the PCM content decreases as a result of leakage.

2. Battery module and problem description

Generally, the battery temperature increases during operation of EVs as a result of heat generation inside the battery. Battery system requires thermal management to prevent thermal runaway while ensuring better capacity, stability and lifecycle. Figure 1 depicts the geometry and proposed thermal management system of the battery module. The battery pack consists of nine prismatic LiFePO$_4$ cells integrated with PCM leaving airgaps at the top of the cells. The specification of the selected battery is summarized in Table 1 (Yunyun et al., 2014). The Ev is assumed to drive for 60 minutes at 2C discharge rate. The PCM shrink level is denoted as Φ and the PCM thickness around a cell is symbolized as L and M. The PCM serves as heat sink by absorbing the heat generated in the battery, and the airgap functions as a medium for air circulation. Two rakes are defined; a mid-horizontal rake (R_h) located at X ϵ [0 147] mm, Y = 281.5 mm, and a vertical rake (R_v) at a location X = 51 mm, Y ϵ [0 563] mm.

3. Mathematical modelling

In Li-ion batteries, the heat released via Joule effect and electrochemical reactions are the two primary heat sources (Ianniciello et al., 2018). Considering a constant discharge rate, a uniform heat generation is presumed inside the battery. The heat generated inside the battery passes on to the PCM and dispersed throughout the module by conduction for the passive thermal management system. The heat transferred to the ambient takes place through convection at the boundary of the battery module. A 2D module of the problem is developed and meshed using ICEM software. A commercial computational fluid dynamic software ANSYS FLUENT was employed to solve the governing conservation equations. A conjugate heat transfer is adopted for the stated problem with natural convection coefficient h = 7 W/m^{2}K around all surfaces and ambient temperature T_{amb} = 298 K. The assumptions, initial and boundary conditions are as follows:

(a) Assumptions
- Thermophysical properties are uniform and isotropic except for the thermal conductivity.
- An orthotropic thermal conductivity is considered for the cells.
- Heat generation in the cell is constant.
- Initial temperature of the cells and ambient temperature are the same (298 K).
- No flow occurred for the liquid PCM.
- Radiation effect is neglected.

(b) Initial and boundary conditions

$$t = 0, \qquad T(x,y) = T_0 \tag{1}$$

$$-k_{cell}\frac{\partial T_{cell}}{\partial n} = -k_{PCM}\frac{\partial T_{PCM}}{\partial n} \tag{2}$$

$$-k_{PCM}\frac{\partial T_{PCM}}{\partial n} = h(T_{PCM} - T_{amb}) \tag{3}$$

(i) For airgap module

$$-k_{cell}\frac{\partial T_{cell}}{\partial n} = h(T_{cell} - T_{airgap}) \tag{4}$$

$$-k_{PCM}\frac{\partial T_{PCM}}{\partial n} = h(T_{PCM} - T_{airgap}) \tag{5}$$

(ii) For aluminum module

$$h(T_{airgap} - T_{Al}) = -k_{Al}\frac{\partial T_{Al}}{\partial n} \tag{6}$$

$$-k_{Al}\frac{\partial T_{Al}}{\partial n} = h(T_{Al} - T_{amb}) \tag{7}$$

In the present study, the numerical simulations based on finite volume method are performed in order to investigate the thermal behavior of the cells. The enthalpy-porosity technique is adopted to deal with the liquid/solid phases during the melting process of the PCM. To select a PCM for battery thermal management.
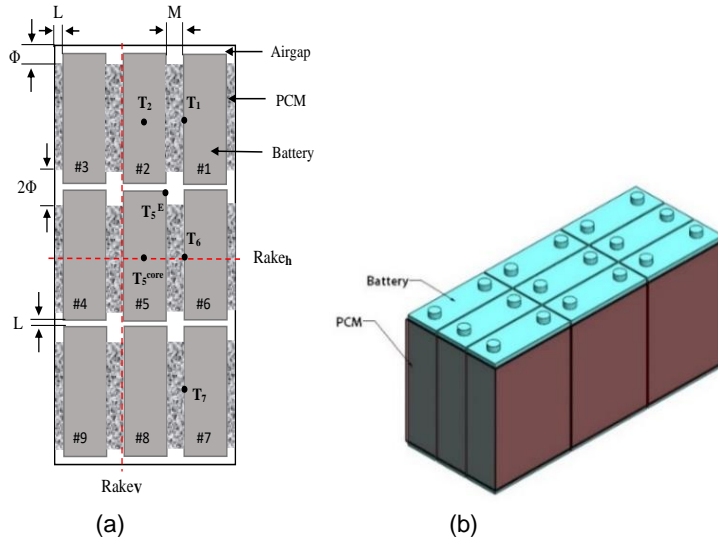

Figure 1: Battery module outline with airgap (a) schematic and (b) 3D view

Table 1: Selected battery specifications (Yuyun et al., 2014)

Property	Specification
Nominal voltage	3.2 V
Capacity	50 Ah
Specific heat	876 ($Jkg^{-1}K^{-1}$)
Thermal conductivity	K_{xx}/K_{yy} = 0.895/2.605 ($Wm^{-1}K^{-1}$)
Density	2,000 (kgm^{-3})
Dimension	120 x 45 x 185 (mm)

The physical and chemical properties of the material should be considered. The important parameters such as melting temperature and latent heat of fusion are to be considered. Table 2 summarized the specifications of the PCM/EG (Wu et al., 2018) used in this study. For each domain (cell, PCM, airgap and aluminum sheet), the governing equations are summarized as:

$$\rho_{cell}C_{p,cell}\frac{\partial T_{cell}}{\partial t} = \nabla(k_{cell}\nabla T_{cell}) + Q \tag{8}$$

$$\rho_{\theta}C_{p,\theta}\frac{\partial T_{\theta}}{\partial t} = \nabla(k_{\theta}\nabla T_{\theta}) \tag{9}$$

where θ can be PCM, airgap or aluminum sheet.

Table 2: PCM/EG specification (Wu et al., 2018)

Property	Specification
Density	950 (kgm^{-3})
Specific heat	3,000 ($Jkg^{-1}K^{-1}$)
Thermal conductivity	7 ($Wm^{-1}K^{-1}$)
Melting heat	148,000 (Jkg^{-1})
Solidus/Liquidus temperature	315.15/317.15 (K)

4. Results and discussion

4.1 Grid independence and model validation

A test for grid independence was carried out for coarse, medium and fine grid to validate the mesh size by generating 60,372, 86,955 and 132,810 cells. The temperature profile along the vertical rake (R_V) is chosen as the convergence criteria. The medium grid (86,955 cells) is selected in this work. Moreover, to ensure accurate and definite simulation process, a model validation was performed and compared with a previous work (Wu et al., 2018). A good agreement between the current prediction and experimental work in Ref. (Wu et al., 2018) was achieved. Thus, the current battery model is reasonable to be employed for the subsequent simulations. Figure 2 shows the grid independence test and model validation.
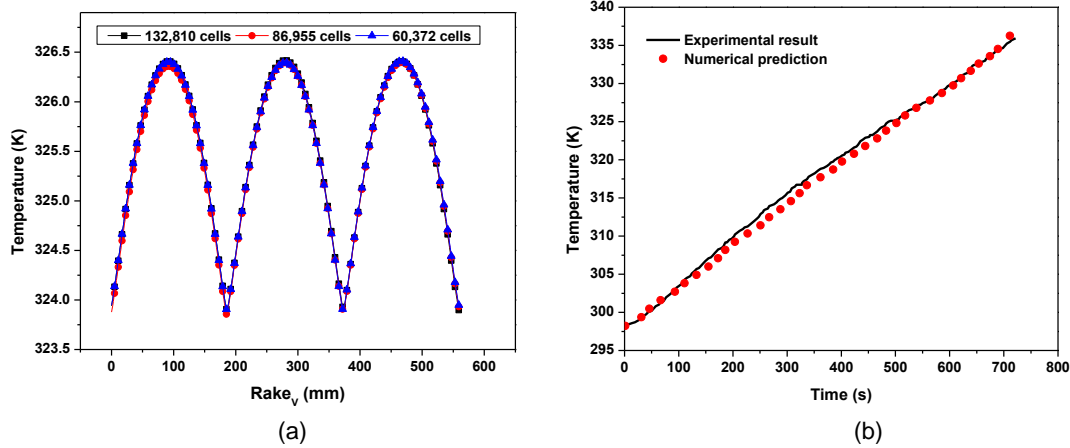

| (a) | (b) |

Figure 2: Temperature profile for (a) grid independence test along the vertical rake (R_v) and (b) comparison of numerical prediction with Wu et al., (2018) experimental work

4.2 Airgap effects on PCM shrink level

To evaluate and compare the effects of airgap on the cells exposed to open and closed medium, the battery pack at normal operation condition with full PCM around the cells (reference configuration) is first studied. Considering the horizontal rake (R_h) created along the mid height of the module, the temperature distribution at the peak locations (from X=56 mm to 90 mm) comparing the opened and closed medium configurations is depicted in Figure 3. It can clearly be distinguished that, the opened medium configuration diminished the maximum temperature raise compared to the closed medium one at different PCM shrink levels. As the PCM shrink level increase, the temperature is found to be increasing. This is due to the decrease of heat absorption and dissipation mode by the PCM. At the end of discharge, the percent increase of temperature for open medium configuration were 0.01 %, 0.03 % and 0.04 % for Φ = 4, 6 and 8 mm compared to Φ = 2 mm. For close medium, the percent increases of temperatures were 0.08 %, 0.16 % and 0.25 % for Φ = 4, 6 and 8 mm compared to Φ = 2 mm. The amount of air circulating at the PCM shrink level add in heat dissipation for the cells and PCM, and will prevent temperature rise. The two important criteria to assess a battery thermal management system are, improving the temperature uniformity and reducing the temperature escalation. Table 3 shows the maximum and minimum temperature in the modules for different configurations at the end of discharge.

4.3 Aluminum and contact resistance effect on heat transfer

A contact resistance (R_c), which occurs as a result of surface roughness between different layers can be significant/insignificant. In the current work, an aluminum of different thickness is placed at the top of the battery pack, and thus may affect the heat transfer rate. For aluminum with thickness L, the contact resistance (R_c) is given as:

$$R_c = \frac{\Delta T_{\text{int }erface}}{\dot{q}}$$

(10)

where $\dot{q}$ is the heat flux at the interface. The contact resistance for aluminum interface (10 μm surface roughness, 10^5 Nm^{-2}) and having air as the interfacial fluid is 2.75×10^{-4} m^{2}KW^{-1} (Bergman et al., 2011). The contact resistance value in the current work is insignificant in the simulation results.
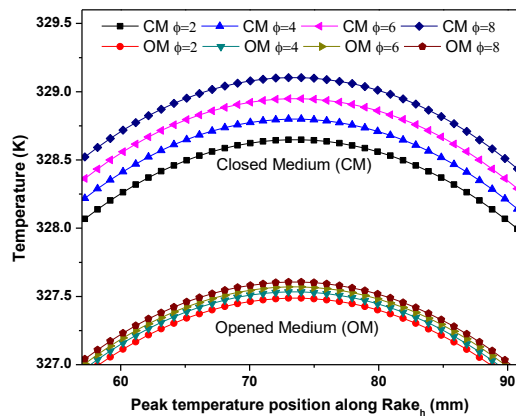
Figure 3: Temperature profile along the horizontal rake

Table 3: Critical temperature in the modules for different configurations

Configurations	Minimum temperature (K) Flow time 60 min	Maximum temperature (K) Flow time 60 min
Open medium		
Φ = 2 mm	323.913	327.489
Φ = 4 mm	323.693	327.535
Φ = 6 mm	323.542	327.571
Φ = 8 mm	323.430	327.607
Close medium		
Φ = 2 mm	327.531	328.661
Φ = 4 mm	327.714	328.931
Φ = 6 mm	327.832	329.199
Φ = 8 mm	328.005	329.467

In order to increase the heat dissipation area, aluminum with different thickness (1, 2, and 3 mm) is employed. Three different configuration were compared; all PCM without leakage (as a reference configuration), PCM – airgap (having leakage), and PCM – airgap – Al (leakage configuration with aluminum on top). Table 4 illustrated the effect of aluminum on top of the battery pack. Comparing the PCM – airgap configuration with that of PCM – airgap – Al, the latter decreases the maximum temperature than the former. This is due to the increase in heat dissipation area by the aluminum. Increasing the aluminum thickness led to the decrease in temperature in the battery modules, however manufacturing standard should be followed to avoid overweighing the battery modules.

Table 4: Critical temperature in the modules for different configurations

Configurations	Minimum temperature (K) Flow time 60 min	Maximum temperature (K) Flow time 60 min	Average temperature (K) Flow time 60 min
PCM only	319.887	326.457	324.007
PCM-airgap	320.061	327.375	325.456
PCM-airgap-Al 1 mm	320.045	327.295	325.372
PCM-airgap-Al 2 mm	320.021	327.153	325.232
PCM-airgap-Al 3 mm	320.011	327.081	325.155

4.4 Charge/discharge cycles

In this section, dynamic cycles test was performed to further analyse the thermal performance of the proposed model. A 5C discharge rate (Q = 52.835 kWm^{-3}) and 0.5C charge rate (Q = 4.680 kWm^{-3}) were considered. A 3 mm thick aluminum is selected. The ambient temperature and heat transfer coefficient used were 303 K and 10 Wm^{-2}K^{-1}. Usually, the generated heat in the cells is absorbed and stored in the PCM as latent heat. The stored heat should be effectively dissipated to the ambient otherwise, it will accumulate and result in higher initial temperature for the subsequent cycle. The maximum temperature at the end of 1st, 2nd, 3rd and 4th discharge for PCM – airgap configuration is 316.645 K, 340.479 K, 354.592 K and 363.305K. For the PCM – airgap – Al 3 mm, the maximum temperature at the end of the respective discharge is 316.495 K, 339.469 K, 353.422 K and

361.995 K. The PCM – airgap – Al 3 mm configuration decreases the temperature by 0.15 K, 1.01 K, 1.17 K and 1.31 K for 1st, 2nd, 3rd and 4th discharge in comparison with PCM – airgap configuration. This indicate that, placing aluminum at the top of the battery modules is beneficial and can decrease the temperature during a severe operation condition.

5. Conclusions

In the current work, thermal performance of a two-dimensional model of a prismatic Li-ion battery modules is evaluated under severely operation condition. Two different configurations describing some part of the cells are exposed due to PCM leakage: one with the top of the cells exposed to open medium with free air convection and the other, with the top of the cells exposed to close medium with no air circulation. At different PCM shrink levels Φ = 2, 4, 6 and 8 mm, the open medium configuration, decreases the temperature in the modules by 1.172 K, 1.396 K, 1.628 K and 1.860 K, compared to the close medium configuration. Placing an aluminum sheet on the battery modules increases temperature uniformity and decreases the maximum temperature. Increasing the aluminum thickness results in decreasing the temperature however, a manufacturing guide and standard should be followed to avoid overweighing the battery modules. For the charge/discharge cycles, the PCM – airgap - Al 3 mm configuration decreases the maximum temperature in the battery modules by 1.31 K compared to the PCM – airgap configuration. Using an aluminum sheet and air circulation at the PCM shrink level can improve the thermal performance of battery module under severely operation condition. In the future work, a cost analysis, and employing a heat pipe in the module to further dissipate the generated heat will be considered.

References

Al-Hallaj S., Selman J.R., 2000, A novel thermal management system for electric vehicle batteries using phase-change material, Journal of the Electrochemical Society, 147, 3231-3236.

ANSYS, Inc., 2016, ANSYS Fluent users' guide, release 17.2.

Bergman T.L., Lavine A.S., Incropera F.P., Dewitt D.P., 2011, Fundamentals of heat and mass transfer, John Wiley & Sons, Incorporated, USA.

De Wilde H.PJ., Kroon P., 2013, Policy options to reduce passenger cars CO_2 emissions after 2020. ECN. ECN-E-13005.

Ferrero E., Alessandrini S., Balanzino A., 2016, Impact of the electric vehicles on the air pollution from a highway, Applied Energy 169, 450-459.

Ianniciello L., Biwole P.H., Achard P., 2018, Electric vehicles batteries thermal management system employing phase change materials, Journal of Power Sources 378, 383-403.

Javani N., Dincer I., Naterer G.F., Yilbas B.S., 2014, Heat transfer and thermal management with PCMs in a Li-ion battery cell for electric vehicles, Intl. Journal of Heat and Mass Transfer 72, 690-703.

Kim J., Oh J., Lee H., 2019, Review on battery thermal management system for electric vehicles, Applied Thermal Engineering 149, 192-212.

Li H., Chen H., Li X., Sanjayan J.G., 2014, Development of thermal energy storage composite and prevention of PCM leakage, Applied Energy, 135, 225-233.

Luo J., Zeng Y., 2017, Research on development of the lithium-ion battery, Chemical Engineering Transactions, 62, 97-102.

Matthias D., Frederic R., 2018, Policy options for a decarbonisation of passenger cars in the EU: Recommendations based on a literature review, Wuppertal Papers, No. 193.

Wang J., Kang L., Liu Y., 2019, Effects of working temperature on route planning for electric bus fleets based on dynamic programming, Chemical Engineering Transactions, 76, 907-912.

Wu W., Wu W., Wang S., 2017, Thermal optimization of composite PCM based large-format lithium-ion battery modules under extreme operating conditions, Energy Convers Manage 153, 22-33.

Wu W., Wu W., Wang S., 2018, Thermal management optimization of a prismatic battery with shape-stabilized phase change material, Int. Journal of Heat Mass Trans, 121, 967–977.

Yuyun Z., Guoqing Z., Weixiong W., Weixiong L., 2014, Heat dissipation research for rectangle $LiFePO_4$ power battery. Heat Mass Transfer, 50, 887–893.